

Determination Overlapping Interface Structure in the ξ' -Al-Ni-Rh Approximant Phase

Yadi ZHAI, Wenhan ZHANG, Yanhui CHEN*

Institute of Microstructure and Property of Advanced Materials, Beijing University of Technology, Beijing, China

crossref <http://dx.doi.org/10.5755/j02.ms.24519>

Received 28 June 2019; accepted 23 January 2020

The structure of the overlapping interface in ξ' -Al-Ni-Rh was determined by calculating the total energy of super lattices containing defect structures using the modified analytic embedded-atom method (MAEAM). The structure analyses indicated that only two equivalent types of interfaces exist, which are defined as the PF and PI types. Calculation of the PF- and PI-type super cells indicated that the interface between the close-packed P layer and the slightly puckered I layer has a lower energy and may be a static interface. Although the PI-type overlapping interface may seriously corrupt decagonal cluster columns in the approximant phase, it causes relatively less corruption of the metallic bonds than the PF mode. The total energies of the three types of super lattices caused by different displacement vectors between the two domains found in ξ' -Al-Ni-Rh were also calculated. The domain boundary translated with a vector of $\mathbf{r} = \frac{1}{2}\mathbf{a} + \frac{1}{2\tau}\mathbf{c}$ is the most static state among the three type super lattices from energy perspective.

Keywords: Al-Ni-Rh approximant phase, interface, total energy, MAEAM, decagonal cluster column.

1. INTRODUCTION

The ξ' -Al-Ni-Rh phase is an intermetallic complex phase and usually coexists as an approximant phase with quasicrystals. The typical complex phase has giant unit cells containing hundreds to thousands of atoms [1]. As a special type of crystal with large numbers of atoms as repeating units, the approximant phase has intrinsic defects, including elemental variations and structural defects. Studies on defect structures in complex phase alloys can aid in our understanding of their formation mechanism and their relationship with quasicrystals.

The key factors affecting material properties are based on surface or interface structures. Experimental information on the detailed atomic structure, especially the segregation of elements and dislocation information, can be obtained by HRTEM (high-resolution electron microscopy) studies of the interface. Furthermore, if molecular dynamics calculations from an energy perspective are available, information on both the structure and energy can provide researchers with a new view of the materials and can guide potential practical applications of such materials for a wide variety of fields.

In our previous work, we reported a HRTEM (high-resolution transmission electron microscopy) study on network domain boundaries, in which the formation of the structure can be regarded as an overlapping of adjacent domains with special translation operations [2]. However, there remained a question regarding the layer at which the two domains translate and then overlap to form a special structure. The quasicrystal phase and defected approximant

phase have similar structures, and determining the defect structure in the approximant phase is important and meaningful for us to understand their relationships and formation mechanism. In the following section, an energy calculation using molecular dynamics simulations will be conducted to define translation interfaces, and the interfaces with the lowest energies will be illuminated from an energy perspective.

2. MOTIVATION AND CALCULATION METHOD

Fig. 1 a–c shows HRTEM images of three types of domain boundaries [3]. The inner part of the domain exhibits a typical ξ' phase structure. At the boundary identified by an arrow in Fig. 1, a different structure with dimmer dots can be seen compared to the base regions. The special boundaries are formed by the overlapping of two domains after translation operations. Fig. 1 d–f gives a schematic illustration of the two domains projected along the [010] direction, where new unit cells are drawn as squares. In the schematic illustration, the bold and dashed lines represent tilings of the two adjacent overlapping domains. The arrows represent two translation vectors with $\mathbf{r} = \frac{1}{2\tau}\mathbf{a} + \frac{1}{2\tau^2}\mathbf{c}$; $\mathbf{r} = \frac{1}{2}\mathbf{a} + \frac{1}{2\tau}\mathbf{c}$; $\mathbf{r} = \frac{1}{2\tau^2}\mathbf{a} + \frac{1}{2}\mathbf{c}$ from left to right, respectively. We defined the three types of domains as A (Fig. 1 a), B (Fig. 1 b) and C (Fig. 1 c) type boundaries, respectively. Structural HRTEM simulations using JEMS indicated perfect consistency with the experimental results [3].

* Corresponding author. Tel.: +86-10-67396521.
E-mail address: yhchen@bjut.edu.cn (Y. Chen)

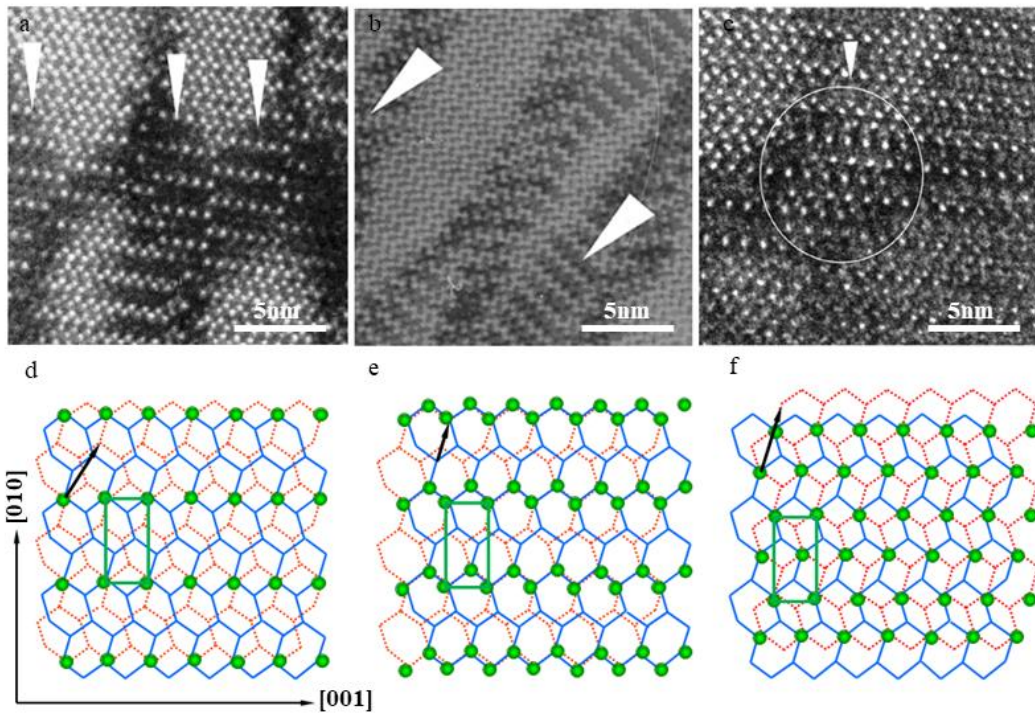


Fig. 1. a, c—HRTEM [3] images of three types of domain boundaries. Arrowheads indicate the super lattice; d, f—tilings of CSL overlapping models. Bold blue lines represent one domain, and dashed orange lines represent another, in which the green square represents the smallest unit of each type, the arrows indicate the displacement vector, and the green balls represent the bright dots shown in the HRTEM images

The ξ' -Al-Ni-Rh phase has a long periodicity of 16 Å along the b direction and tends to form defect structures due to tiny environmental vibrations in the solidification process. Hopping of the half cluster column becomes available based on structural considerations. The translation vectors in the a-c plane were determined by HRTEM results. A determination of the interface of the overlapping/slipping layer is also necessary for understanding the formation mechanism.

A detailed atomic structure of ξ' -Al-Ni-Rh indicates that there are three basic/effective layers viewed in the b-c plane, while five other layers can be obtained by mirror or inverse symmetry operations. As shown in Fig. 2, three basic atomic layers can be indexed as I, P and F layers. The footnote “i” represents an inverse symmetry operation, and “*” represents a mirror operation. Based on crystallographic

principles, an interface usually lies on close-packed layers, which have the weakest bonding forces with other layers. The P/P*/Pi* layer in ξ' -Al-Ni-Rh is a close-packed layer compared with the other layers and it tends to be exposed to the environment as a surface or interface [4]. Fournee’s work on the ξ' -Al-Pd-Mn phase, which has the same structure as the ξ' -Al-Ni-Rh phase, indicated that its surface appears as a step-like structure with a P layer exposed on the surface [5]. Thus, there are only two types of possible interfaces: an interface of type I, between a P layer (close-packed layer) and an I layer (relaxation layer and symmetric center), and an interface of type II, between a P layer (close-packed layer) and an F layer (flat layer). Other types of interfaces can be regarded as equivalent to the above two types.

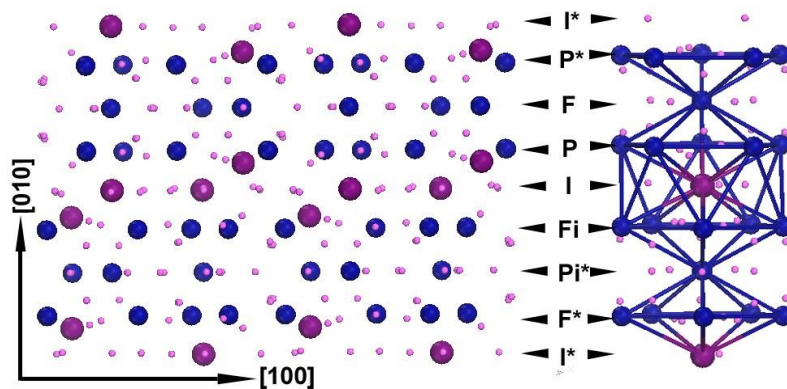


Fig. 2. The left figure shows a projection of the structure of the ξ' -Al-Ni-Rh phase in the a-b plane, representing the layered structure along the b direction; a key identifying the layers is provided in the middle of the figure. The right figure is the basic building cluster column, with two rotated icosahedrons connected by one Rh atom

According to the model shown in Fig. 1 d and our analysis of the atomic structure of ξ' -Al-Ni-Rh, two atomic models were constructed, as shown in Fig. 3 for the a–c plane.

The two models contain 16 atomic layers along the b direction, which is twice the unit length of the original ξ' -Al-Ni-Rh phase. The two types of interfaces were indexed as PF and PI types based on the overlapping interface layers. Although the boundaries are different, the projections along the b direction have the same structures. Fig. 3 shows the atomic models in the a-c plane and one typical cluster illustrated by bond connections. The lattice parameters are as follows: $a = 23.54 \text{ \AA}$, $b = 33.12 \text{ \AA}$, $c = 12.56 \text{ \AA}$, $\alpha = \beta = \gamma = 90^\circ$.

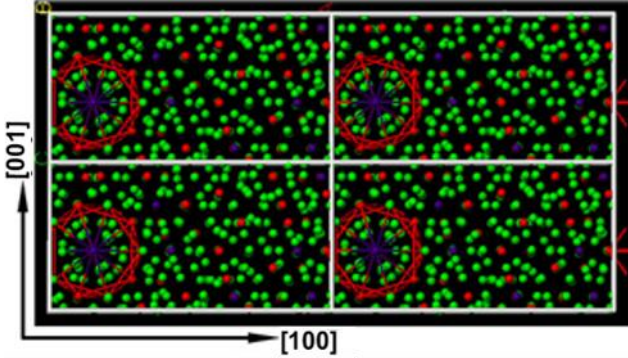


Fig. 3. Atomic structure of the PF-type super unit with a $2 \times 1 \times 2$ structure along the b direction (which has the same atomic structure as a PI-type super unit in the same observation direction). The parameters of the model are $a = 23.54 \text{ \AA}$, $b = 33.12 \text{ \AA}$, $c = 12.56 \text{ \AA}$, $\alpha = \beta = \gamma = 90^\circ$

To eliminate any surface effects, the translated part was chosen to be embedded in the center of the super cell. Fig. 4 shows the two types of super unit cells viewed in the a–b plane, in which red balls represent the translated part while green balls represent the untranslated part. Fig. 4 a shows the model of the interface between the P and F layers (PF), and Fig. 4 b shows the model of the interface between the P and I layers (PI). Clusters are a special and basic unit in quasicrystals and approximant phases, and their integrity usually needs to be considered. The formation of a PF-type interface damages the top of the cluster, as shown in Fig. 4 a.

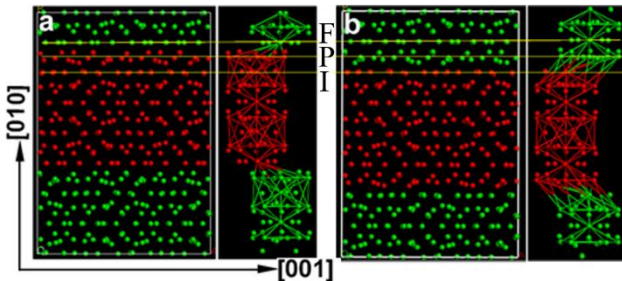


Fig. 4. Two types of atomic models caused by different overlapping modes with 16 layers and corresponding clusters. The red balls represent atoms that have changed position, and green balls represent atoms that have not changed position. a – interface between P and F layers (PF); b – interface between P and I layers (PI)

The formation of a PI-type interface translates the cluster from the middle of the column (Fig. 4 b), thus damaging the cluster more seriously than the PF type.

A determination of the overlapping interface can clarify the role of clusters in the formation of quasicrystals and their approximants. The difference in the two types of interfaces can only be discerned from the $\langle 001 \rangle$ or $\langle 100 \rangle$ directions, as shown in Fig. 4 and Fig. 5. However, it is very difficult to obtain experimental HRTEM data by tilting a sample in a microscope due to the small sample area, which is less than 5 nm^2 . It is known that low-energy stable structures have a higher probability of existing in alloys than high-energy structures. Thus, an energy consideration can be employed to solve the problem. A molecular dynamics calculation was conducted to achieve this goal due to the large unit cells with hundreds of atoms.

Molecular dynamics calculations are usually applied to multi-atom systems containing hundreds of atomic nuclei and electrons. The calculation simulates the movement trajectories of the nuclei to optimize the system's structure and properties. In the calculation process, each nucleus is regarded as moving in a typical Newtonian force field created by all other nuclei and electrons. Essentially, an initial state is defined, and then the atoms move, constrained by the force field. Eventually, the total energy is recorded along with its time dependence. The key step in obtaining reliable calculation results is choosing a suitable force field. The EAM (Embedded Atomic Method) is based on the electronic density function and has been successfully applied to systems such as metals, alloys and rare metals. The EAM has also been successfully applied to special systems such as solid phonons, defect structures, alloys, doping structures, surface adsorptions and diffusions [6]. A modified analytical EAM [7] force field was used in our work to calculate the total energy of the two structures, and the total energy of a system containing N atoms is

$$E_{\text{tot}} = \sum E_i, \quad (1)$$

$$E_i = \frac{1}{2} \sum_{j \neq i} \phi(r_{ij}) + F(\rho_i) + M(P_i), \quad (2)$$

where E_{tot} is the total energy of the system, ρ_i is the total density of the electrons, r_{ij} is the distance between atoms i and j , $F(\rho_i)$ is the embedded energy when one atom is embedded into an area with an electronic density of ρ_i , $\phi(r_{ij})$ is the interaction between atoms i and atom j , and $M(P_i)$ is the modified energy.

3. RESULTS AND DISCUSSION

The relationship between the total energy and steps or time processing is illustrated in Fig. 5, in which the bold line represents the variation in the total energy of a PI-type super unit while the dashed line represents the total energy of a PF-type super unit. The inset shows an enlargement of the energy variation for the first 5 steps. The total energy analysis indicates that the energy of the PI-type super unit, for both the original (0 step) and stable structure (after 60000 steps), is smaller than the energy of the PF-type super unit. This result indicates that the overlapping interface between the P and I layer has a higher probability of existing

in ξ' -Al-Ni-Rh phases than the interface between the P and F layers. Thus, we can infer that the interface in Fig. 1 b and 1c also occurs between P and I layer.

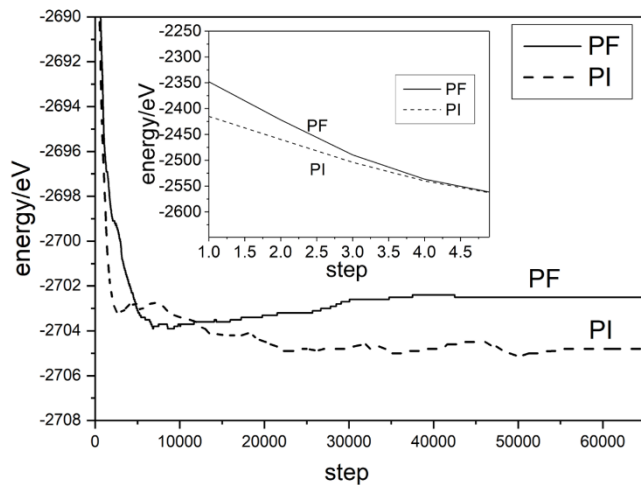


Fig. 5. Energy variance before and after relaxation of the two model types, in which the bold line represents the energy variance of the PI boundary and the dashed line represents the energy variance of the PF boundary. The inset image shows the energy variance of the initial stage of the two systems

Based on the above model and analysis, B- and C-type super units with a PF overlapping interface were also constructed, and their total energies during the relaxation process were compared. The relationship between the total energy and steps is shown in Fig. 6, in which squares, balls and triangles represent A-, B- and C-type super units, respectively. The inset shows the total energy for the first 5 steps.

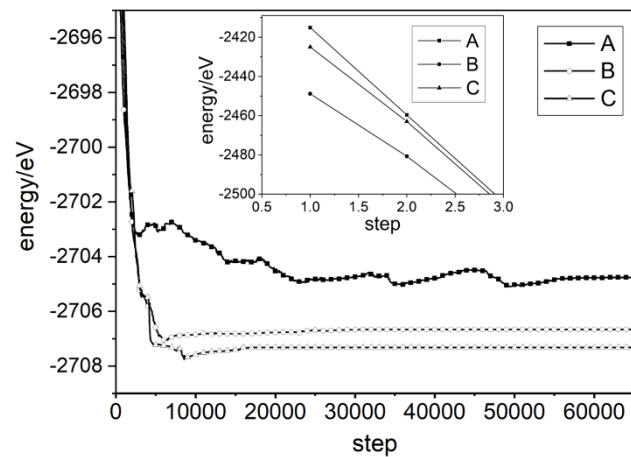


Fig. 6. Energy variance before and after relaxation of the three model types in the domain boundaries. The squares, circles and triangles represent the energy variances of the A-, B- and C-type models. The inset image shows the initial energy variance

From the above calculation and analysis, the formation of the most likely overlapping model, as determined from an energy perspective, significantly damages the clusters. Thus, we can infer that in addition to the perfection of the cluster, the bonding energy between atoms in the quasicrystals and approximant phases should be considered. The PF-type boundary in Al-Ni-Rh approximant phases

maintains the integrity of the clusters better than the PI-type boundary from a structural perspective. However, there is an additional convex Al atom layer between the P and F layers, as shown in Fig. 2, and the quantity of total atoms in the F layer plus these Al atoms is greater than that in the I layer. The bonding between the P and F layers is stronger than the bonding between the P and I layer; thus, the total energy of the PI-type super unit is weaker than that for the PF-type super unit.

As a special type of defect structure, the formation of a CSL (coincidence site lattice) boundary structure can diminish the total energy by altering fewer atoms in comparison to other types of boundaries. The CSL boundary is the most common structure in defect regions [8, 9]. The formation of a CSL structure in the Al-Ni-Rh phase can reduce the total energy and can produce many coincidence sites between two adjacent domains. To some degree, the CSL boundary prompts the formation of quasicrystal structures and coincides with the coverage model of quasicrystal materials. CSL boundaries in the Al-Ni-Rh approximant phase show the strong relationships between quasicrystals and approximant phases [10], and also present the lowest total energy from a theoretical perspective.

4. CONCLUSIONS

The structure of an overlapping interface was determined by calculating the total energy of super cells using a molecular dynamics method based on the modified analytic embedded-atom method (MAEAM). Structural analyses indicate that PI and PF, which are two overlapping interface types, can be possibly and effectively existent. Interfaces between the close-packed P layer and the puckered symmetric center I layer are higher in probability due to their lower total energy. Although a PI-type boundary damages the clusters more seriously than a PF-type boundary, the former corrupts fewer bonds. The comparison of the three types of coincidence site lattice overlapping boundary types indicates that the boundary resulting from the phason translation mode has the lowest energy. The combination of HRTEM and molecular dynamics calculations based on EAM can provide a detailed structure of nano-scale domain boundaries. This method can be very helpful for material researchers for complex structural optimization and confirmation.

Acknowledgments

This work was supported Natural Science Foundation of China in grants (No. 91860202, No.51872008) and Beijing Natural Science Foundation (No.1182005, No. Z180014) and “111” project under the grand of DB18015 and Beijing Outstanding Young Scientists Projects (BJJWZYJH01201910005018). The authors thanks Dr. Dongchang Wu from Thermofisher Scientific Shanghai Nanopoint for useful discussion and assistance in Titan-ETEM and Titan-Themis.

REFERENCES

1. **Urban, K., Feuerbacher, M.** Structurally Complex Alloy Phases *Journal of Non-Crystalline Solids* 334 2004: pp.143 – 150.

<https://doi.org/10.1016/j.jnoncrysol.2003.11.029>

2. **Chen, Y.H., Sun, W., Zhang, Z.** Approximant Phases, Phason Planes and Domain-Boundary Networks in Al-Ni-Rh alloys *Philosophical Magazine Letters* 86 (12) 2006: pp. 817 – 827.
<https://doi.org/10.1080/09500830601057934>
3. **Chen, Y.H., Sun, W., Zhang, Z.** On Electron Microscopy Study of Special Planar Defects in Al-Ni-Rh Complex Alloys *Journal of Chinese Electron Microscopy Society* 26 (4) 2007: pp. 288 – 297.
[https://doi.org/10.1016/S1872-2040\(07\)60040-1](https://doi.org/10.1016/S1872-2040(07)60040-1)
4. **Friedel, J.** Dislocations. Pergamon, 1964.
5. **Fourniee, V., Rose, A.R., Lograsso, T.A., Anderegg, J.W., Dong, C., Kramer, M., Fisher, I.R., Canfield, P.C., Thie, P.A.** Surface Structures of Approximant Phases in the Al-Pd-Mn System *Physical Review B* 66 (16) 2002: pp. 165423 – 1.
<https://doi.org/10.1103/PhysRevB.66.165423>
6. **Zhang, B.W., Hu, W.Y., Shu, X.L.** Theory of Embedded Atom Method and its Application to Material Science-Atomic Scale Materials Design Theory, Changsha: Hunan University Press, 2002.
7. **Hu, W.Y., Zhang, B.W., Huang, B.Y.** Recent Development and Prospects for the Analytic EAM model *Rare Metal Materials and Engineering* 28 1999: pp. 1 – 9.
8. **Yang, S.H., Ding, D.-H.** Dislocation Theory of Crystal. Beijing: Science Press, 1998: 176.
9. **Bollman, W.** Crystal Defect and Crystalline Interface. Berlin: Springer, 1970.
https://doi.org/10.1007/978-3-642-49173-3_11
10. **Kuo, K.H.** Quasiperiodic crystals. Hangzhou: Zhejiang Science and Technology Press, 2006.



© Zhai et al. 2021 Open Access This article is distributed under the terms of the Creative Commons Attribution 4.0 International License (<http://creativecommons.org/licenses/by/4.0/>), which permits unrestricted use, distribution, and reproduction in any medium, provided you give appropriate credit to the original author(s) and the source, provide a link to the Creative Commons license, and indicate if changes were made.